B. KUROWSKI©[1]*, D. OLESZAK©[1]

INFLUENCE OF ALUMINIUM AND SILICON CONTENT ON THE PHASE COMPOSITION, MICROSTRUCTURE AND MAGNETIC AND MECHANICAL PROPERTIES OF MULTICOMPONENT FeNiCoAlSi ALLOYS

This work deals with the characterization of structure, magnetic and mechanical properties of $(FeNiCo)_{100-x}(AlSi)_x$ ($x = 0, 5, 10, 15, 25$) multicomponent alloys prepared by casting. The results of X-ray diffraction measurements, scanning electron microscopy observations and hardness and magnetic properties investigations are presented. The studies show that cast $(FeNiCo)_{100-x}(AlSi)_x$ alloys reveal dendritic morphology and their phase composition depends on (Al + Si) content. For $x \leq 10$ a face-centered cubic phase is observed, while the increase of Al and Si content results in a body-centered cubic phase formation. It leads to a fivefold increase of hardness from 88 HV to 526 HV. The investigated alloys have high magnetic induction reaching 170 emu/g, while their coercivity value is even up to 2.9 kA/m for $x = 15$, and strongly depends on chemical and phase composition.

Keywords: multicomponent FeNiCoAlSi alloys; phase composition; microstructure; hardness; magnetic properties

1. Introduction

Scientific and technological progress creates a demand for new materials which allow more efficient work of different devices. The possible way to meet these demands is a modification of already existing materials. An important group of modern materials that needs enhancement are ferromagnetic alloys [1]. Ferromagnetic materials can be divided into magnetically hard materials, like NdFeB and AlNiCo alloys, and magnetically soft materials with low coercivity [2,3]. Soft magnetic materials have been studied for many years due to their high demand in industry. They are easy to magnetize and demagnetize and are used in the electronics industry, for example, crystalline Fe-Si alloys [4]. They have a relatively low resistivity leading to a large eddy current loss. Amorphous and nanocrystalline soft magnetic materials can be used in high-frequency devices due to their low coercivity and high electrical resistance [5-7]. Liu et al. [8,9] showed that $(FeCoNi)_{0.75}Al_{0.25}$ alloys exhibit high magnetization values ($M_s = 101$ emu/g) and low coercivity ($H_c = 268$ A/m). Zuo et al. [10] found that CoNiMnGa alloys exhibit a low magnetostriction coefficient and a high Curie temperature (T_c). In article [11], the $FeCoNi(CuAl)_{0.8}$ alloy consisting of body-centered cubic (BCC) and face-centered cubic (FCC) phases shows good magnetic and mechanical properties. It was found that the BCC phases exhibit higher magnetization than the FCC phases. In another paper

[12], was shown that the addition of Ga to the $FeCoNi(CuAl)_{0.8}$ alloy can form BCC phases, improves the magnetization of the alloy, increases the remanence value and increases the coercivity. In the next paper, it was shown that the addition of Sn to the FeCoCuNi alloy may hinder the formation of the FCC phase [13] and facilitate the formation of the BCC phase [14]. The magnetic properties strongly depend on the composition. The magnetization decreases almost linearly with the increase of Al and Si content in $FeCoNi(AlSi)_x$ ($0 \leq x \leq 0.8$ in molar ratio) [15]. The development of energy-saving materials with magnetic properties between magnetically soft and hard, but with good mechanical properties, driven by the power industry, remains a challenge [16]. FeNiCoAlSi alloys are a promising group of materials suitable for this type of application [17]. Some of these multicomponent alloys can be classified as high or medium entropy alloys, depending on the value of the entropy of mixing.

2. Materials and methods

The $(FeNiCo)_{100-x}(AlSi)_x$ ($x = 0, 5, 10, 15, 25$) alloys were prepared by arc melting a mixture of pure metals and re-melted five times in a high-purity argon atmosphere to ensure homogeneity. The purity of all elements used was better than 99.8%. A Ti-getter was used during the alloys preparation as an oxygen

[1] WARSAW UNIVERSITY OF TECHNOLOGY, FACULTY OF MATERIALS SCIENCE AND ENGINEERING, WOLOSKA STR. 141, 02-507 WARSAW, POLAND

* Corresponding author: bernard.kurowski.dokt@pw.edu.pl

absorber. The master alloy was cast into copper mould to form a rod with diameter of 3 mm. X-ray diffraction (XRD, Rigaku Mini Flex II) was employed to analyse the phase composition of the alloys. Cu Kα radiation ($\lambda = 0.15418$ nm) was used. XRD data were recorded for 2 theta range of 20-120°, with 0,05° step and counting time of 5 s. The lattice parameters of the FCC and BCC solid solutions formed were calculated applying Nelson-Riley approach [18]. The microstructure and elemental chemical composition maps were obtained by scanning electron microscope (SEM, Hitachi S3500N) with energy-dispersive X-ray spectroscopy (EDS). The samples for SEM observations and EDS analysis were subjected to a standard procedure of grinding, polishing and etching. The saturation magnetization and coercivity were measured at room temperature applying a vibrating sample magnetometer (VSM, Lake Shore) with a maximum field of 2 T. Hardness was measured by the Vickers method with a standard load of 30 kG.

3. Results and discussion

The XRD studies show (Fig. 1) that cast (FeNiCo)$_{100-x}$ (AlSi)$_x$ alloys for $x \leq 10$ are single phase with a face-centre cubic (FCC) structure. The increase of Al and Si content results in body-centre cubic phase (BCC) appearance. For $x = 15$ a mixture of two phases FCC + BCC is observed and the contribution of BCC phase was estimated from the XRD pattern as 15 ± 2 wt. %. Whereas single phase BCC structure is found for $x = 25$. The observed change of phase composition from FCC to BBC solid solution with change of chemical composition (in this case increase of Al + Si content) is typical behaviour reported for high entropy alloys [19]. However, the investigated alloys belong to medium entropy group. For $x = 25$ the calculated value of mixing entropy is 13.05 kJ/mol K, i.e. 1.57 R, where R is a gas constant.
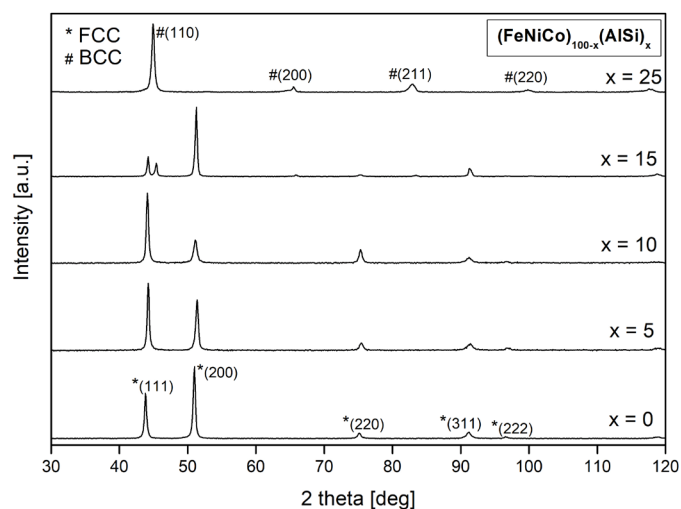

Fig. 1. X-ray diffraction patterns of (FeNiCo)$_{100-x}$(AlSi)$_x$ cast alloys

The increasing of (Al + Si) content influences the value of FCC solid solution lattice parameter. Its value is 0.3580 nm

± 0,0001 nm for $x = 0$ and increases slightly to 0.3582 nm for $x = 5$ and 10, finally reaching 0.3585 nm for $x = 15$. The value of BCC solid solution lattice parameter increases from 0.2848 nm ± 0,0001 nm for $x = 15$ to 0.2850 for $x = 25$.

SEM observations reveal the microstructure of the studied alloys (Fig. 2). For FeNiCo composition rectangular, large grains are visible, around 100 micrometres in size (Fig. 2a). Addition of 5 at. % of (Al + Si) results in significantly smaller grains showing a feature of dendritic morphology, however, not fully developed yet (Fig. 2b). Whereas typical dendritic microstructure is observed for $x = 10$ and 15 (Fig. 2c and d). For $x = 25$ the dendrites seem to be arranged inside typical polygonal grains (Fig. 2e). Generally, the microstructure of the alloys studied become finer with increasing of (Al + Si) content.
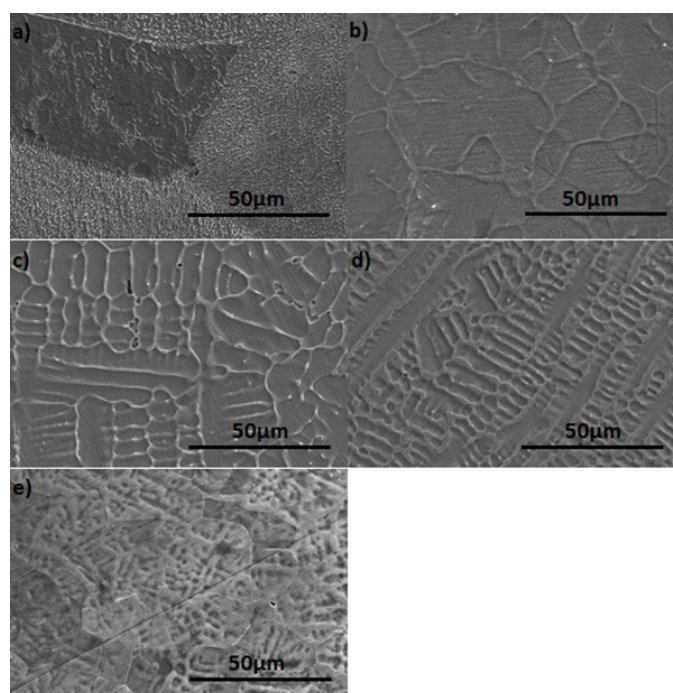

Fig. 2. SEM micrographs showing the microstructure of (FeNiCo)$_{100-x}$ (AlSi)$_x$ alloys for $x = 0$ (a), $x = 5$ (b), $x = 10$ (c), $x = 15$ (d) and $x = 25$ (e)

In order to determine the real chemical composition of the alloys and distribution of the elements, EDS studies were performed. As an example the average composition of the alloy $x = 25$ is given in TABLE 1. The determined composition is in a good agreement with the nominal one.

TABLE 1

Average composition of the FeNiCo)$_{75}$(AlSi)$_{25}$ alloy

Element	at. %	wt. %
Fe	25.46 ± 0.23	28.65 ± 0.26
Ni	23.49 ± 0.35	27.78 ± 0.42
Co	24.12 ± 0.31	28.64 ± 0.36
Al	13.56 ± 0.15	7.37 ± 0.08
Si	13.37 ± 0.14	7.57 ± 0.08
Total	100	100

The mapping of the elements distribution for the alloy containing 25 at. % of (Al + Si) is shown in Fig. 3. Fe, Ni and Co are distributed uniformly in the structure, but the distribution of Al and Si is not fully homogeneous, what is confirmed by a detailed point analysis.
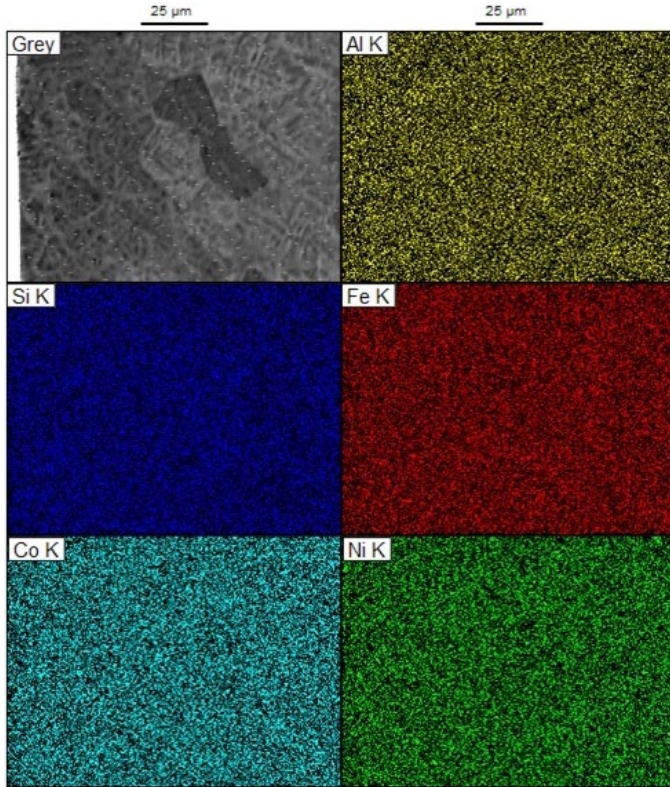

Fig. 3. The distribution of elements for FeNiCo)$_{75}$(AlSi)$_{25}$ alloy

The results of point analysis for the sample $x = 25$ are presented in Fig. 4 and TABLE 2. The distribution of the elements in the dendrites (points 1 and 2) is homogeneous. On the other hand, the interdendritic regions (points 3 and 4) are enriched in Al and simultaneously impoverished in Si.

The magnetic properties measurements show that the investigated alloys have high saturation magnetization in the range from about 170 emu/g (for $x = 0$) to 110 emu/g (for $x = 25$), due to the presence of strong magnetic elements. The decreasing of magnetization with increasing (Al + Si) content is a typical behaviour due to increased content of non-magnetic elements. In the case of coercivity measurements, the dependence of H_c on chemical and phase composition is recorded. With increasing (Al + Si) concentration, the coercivity increases, showing the
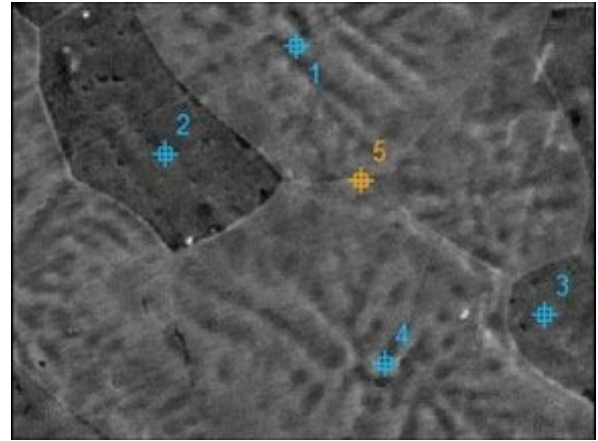

Fig. 4. SEM image of the FeNiCo)$_{75}$(AlSi)$_{25}$ alloy with chemical composition measurements points. The corresponding results are shown in TABLE 2

maximum for $x = 15$, corresponding to the two-phase structure FCC + BCC (Fig. 5). Such a behaviour has been explained as resulting from the possible existence of small precipitations do not detectable by XRD studies [3]. From the magnetic properties point of view the investigated alloys can be classified as semi-hard magnetic materials, revealing the coercivity above 1000 A/m.
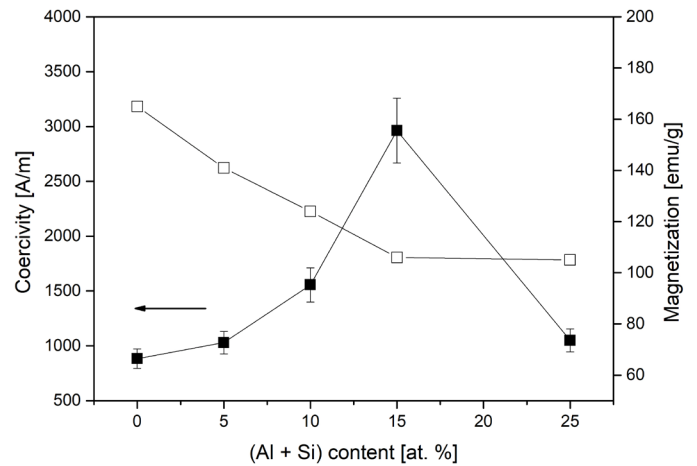

Fig. 5. The changes of coercivity and magnetization for (FeNiCo)$_{100-x}$ (AlSi)$_x$ alloys as a function of (Al + Si) content

The hardness measurements show, that with increasing Al + Si content, the hardness increases from about 100 HV to 600 HV. This is due to the change of the phase composition

TABLE 2

Chemical composition at points marked in Fig. 4

	Fe (at. %)	Ni (at. %)	Co (at. %)	Al (at. %)	Si (at. %)
pt 1	25.19 ± 0.67	24.71 ± 1.01	23.87 ± 0.87	14.31 ± 0.39	11.92 ± 0.21
pt 2	24.72 ± 0.66	22.97 ± 0.99	24.07 ± 0.87	14.58 ± 0.43	13.66 ± 0.41
pt 3	24.66 ± 0.66	23.80 ± 1.02	25.01 ± 0.89	16.26 ± 0.23	10.27 ± 0.19
pt 4	22.74 ± 0.63	26.11 ± 1.01	23.42 ± 0.86	18.02 ± 0.40	9.70 ± 0.20
pt 5	25.65 ± 0.69	24.18 ±1.03	23.84 ± 0.90	11.76 ± 0.22	14.58 ± 0.39

from FCC to BCC. It is known that the hardness of BCC alloys is higher than FCC ones due to their crystallographic structure.
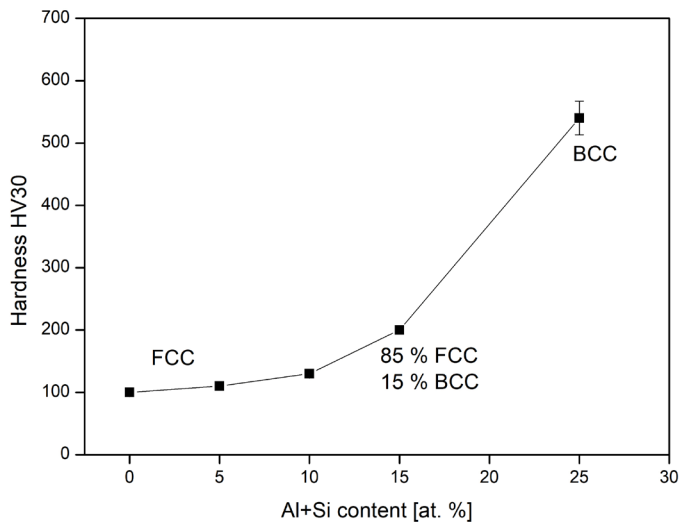

Fig. 6. The hardness of $(FeNiCo)_{100-x}(AlSi)_x$ alloys as a function of (Al + Si) content

4. Conclusions

The performed studies allow to draw the following conclusions:

– the phase composition of the investigated FeNiCoAlSi alloys depends on the chemical composition and changes from FCC to BCC solid solution with increasing Al + Si content,

– the alloys reveal dendritic morphology with segregation of aluminium and silicon,

– the refinement of the microstructure is observed with increased Al + Si concentration,

– the hardness of the alloys increases with Al + Si increase, corresponding to the change from FCC to BCC solid solution,

– the studied alloys belong to semi hard magnetic materials, revealing the changes of magnetization and coercivity with chemical and phase composition.

REFERENCES

[1] M.S. Lucas, L. Mauger, J.A. Munoz, Y. Xiao, A.O. Sheets, S.L. Semiatin, J. Horwath, Z. Turgut, J. Appl. Phys. **109**, 07E307 (2011).

[2] P.P. Li, A.D. Wang, C.T. Liu, J. Alloy. Compd. **694**, 55-60 (2017).

[3] Y. Zhang, T. Zuo, Y. Cheng, P.K. Liaw, Sci. Rep. **3**, 1455 (2013).

[4] B.D. Cullity, C.D. Graham, Introduction to Magnetic Materials, 1st. ed., Addison Wesley, Reading, (1972).

[5] A. Inoue, B.L. Shen, H. Koshiba, H. Kato, A.R. Yavari, Acta Mater. **52**, 1631-1637 (2004).

[6] M.E. McHenry, D.E. Laughlin, Acta Mater. **48**, 223-238 (2000).

[7] G. Herzer, Acta Mater. **61**, 718-734 (2013).

[8] P.P. Li, A.D. Wang, C.T. Liu, Intermetallics. **87**, 21-26 (2017).

[9] P.P. Li, A.D. Wang, C.T. Liu, J. Alloys Compd. **694**, 55-60 (2017).

[10] C. Shang, E. Axinte, W. Ge, Z. Zhang, Y. Wang, Surf. Interfaces **9**, 36-43 (2017).

[11] Q. Zhang, H. Xu, X.H. Tan, X.L. Hou, S.W. Wu, G.S. Tan, L.Y. Yu, J. Alloys Compd. **693**, 1061-1067 (2017).

[12] Z. Li, H. Xu, Y. Gu, M.X. Pan, L.Y. Yu, X.H. Tan, X.L. Hou, J. Alloys Compd. **746**, 285-291 (2018).

[13] L. Liu, J.B. Zhu, C. Zhang, J.C. Li, Q. Jiang, Mater. Sci. Eng. A. **548**, 64-68 (2012).

[14] T. Zuo, M.C. Gao, L. Ouyang, X. Yang, Y. Cheng, R. Feng, S. Chen, P.K. Liaw, J.A. Hawk, Y. Zhang, Acta Mater. **130**, 10-18 (2017).

[15] Y. Zhang, T.T. Zuo, Y.Q. Cheng, P.K. Liaw, Sci. Rep. **3**, 11335e11338 (2015).

[16] G. Da Silveira, N. Slack, Inter. J. Oper. Prod. Manage. **21**, 949-964 (2001).

[17] Z. Li, J. Qi, Z. Li, H. Li, H. Xu, G. Bai, X. Liu, X. Zhang, Mater. Lett. **297**, 129965 (2021).

[18] B.D. Cullity, R.S. Stock, Elements of X-Ray Diffraction, 3rd ed., Prentice Hall, Upper Saddle River (2001).

[19] P. Li, A. Wang, C.T. Liu, Intermetallics **87**, 21-26 (2017).